

Published in final edited form as:

J Am Chem Soc. 2010 April 28; 132(16): 5536–5537. doi:10.1021/ja909148v.

Direct Detection of Nitroxyl in Aqueous Solution using a Tripodal Copper(II) BODIPY Complex

Joel Rosenthal and Stephen J. Lippard

Department of Chemistry, Massachusetts Institute of Technology, 77 Massachusetts Avenue, Cambridge, Massachusetts 02139

Stephen J. Lippard: lippard@mit.edu

Nitric oxide (NO) mediates both physiological and pathological processes.^{1,2} In addition to cardiovascular signaling, NO has been invoked to play a neurochemical role in learning and memory, and it is a powerful necrotic agent wielded by macrophages of the immune system. Whereas considerable effort has been invested to develop metal-based^{3–5} and other^{6,7} probes for detecting nitric oxide, there has been significantly less progress in the synthesis of platforms capable of detecting other reactive nitrogen species (RNS).⁸ Of the nitrogen oxides relevant to biology, nitroxyl (HNO), the one electron reduced, protonated analog of nitric oxide,⁹ is among the least thoroughly investigated.¹⁰ Interest in nitroxyl has grown with the accumulation of evidence that HNO, which has a pK_a of 11.4 and exists primarily in the protonated form under physiological conditions,⁹ displays important biological roles with potential pharmacological applications distinct from those of nitric oxide.^{11–13} For example, HNO reacts directly with thiols,¹⁴ is resistant to scavenging by superoxide,¹⁵ and can activate voltage-dependent K^+ channels in mammalian vascular systems.^{16,17} Moreover, biochemical studies suggest that HNO can be formed directly from nitric oxide synthase under appropriate conditions^{10,18} and that NO and HNO may be able to interconvert in the presence of superoxide dismutase (SOD).¹⁹ Despite accumulating evidence of the biological importance of HNO, studies have been hampered by the lack of a biologically compatible probe for the molecule. Only recently have chemical systems capable of discerning HNO from NO been reported, but the constructs are not suitable for work with biological samples.^{20,21}

Properties required for selective nitroxyl detection using fluorescence methods under physiologically relevant conditions include selectivity over other reactive nitrogen species (RNS) and downstream NO oxidation products, compatibility with living biological samples, water solubility, and membrane permeability. Additionally, incorporation of a signaling moiety with relatively long-wavelength absorption and emission properties is needed to avoid unintended cellular damage by high-energy radiation and to minimize innate biological autofluorescence. BOT1 (Scheme 1) juxtaposes a BODIPY reporter site, which has optical properties that are well suited for cellular imaging experiments,²² with a tripodal dipyrpyridylamine appended receptor via a triazole bridge. The tripodal metal-binding site of BOT1 comprises a tertiary nitrogen bearing two 2-pyridylmethyl substituents. The third arm of the tripod is afforded by the triazole formed upon coupling of an alkyl azide with a terminal alkyne.²³ Accordingly, the triazole arm completes the tripodal coordination environment engendered by the *N*-(triazolylmethyl)-*N,N*-dipicolyl framework while simultaneously providing a rigid spacer between the BODIPY reporter and chelating ligand. This design serves

Correspondence to: Stephen J. Lippard, lippard@mit.edu.

Supporting Information Available: Experimental procedures, characterization data, Table S1, and Figs. S1–S9. This material available free of charge via the Internet at <http://pubs.acs.org>.

to minimize the distance between fluorophore and metal binding site, thereby assuring strong fluorescence quenching in the probe off-state. The triazole arm was installed by the copper(I) mediated click-coupling of alkyne **1** with the azide produced upon in situ displacement of Cl^- from TM-BODIPY- CH_2Cl by NaN_3 .

The photophysical properties of BOT1 were assessed under simulated physiological conditions (50 mM PIPES, 100 mM KCl, pH = 7.0). The probe displays optical properties typical of a BODIPY chromophore, with an absorption band in the visible region centered at 518 nm ($\epsilon = 30,900 \pm 960 \text{ M}^{-1}\text{cm}^{-1}$). Excitation into these bands produces an emission profile with a maximum at 526 nm, and $\Phi_{\text{fl}} = 0.12$ (Fig. 1). Upon addition of one equiv of CuCl_2 to a solution of BOT1, the fluorescence intensity decreased by ~12-fold ($\Phi_{\text{fl}} = 0.01$), which we attribute to photoinduced electron transfer (PET) from the BODIPY singlet excited state to the bound Cu^{2+} ion (Fig. S1, Supporting Information). The positive ion electrospray mass spectrum of this species displayed a peak with $m/z = 638.3$, which corresponds to that of $[\text{Cu}^{\text{II}}(\text{BOT1})\text{Cl}]^+$ (calcd. $m/z = 638.2$) (Fig. S2). Titration of BOT1 with CuCl_2 , produced the series of emission changes displayed in Fig. S3, with an apparent dissociation constant of $K_d = 3.0 \pm 0.1 \text{ }\mu\text{M}$ (Fig. S3), as calculated by a Benesi-Hildebrand analysis. Photophysical data recorded for BOT1 and $\text{Cu}^{\text{II}}[\text{BOT1}]$ are available (Table S1). Analytically pure $[\text{Cu}(\text{BOT1})\text{Cl}]\text{Cl}$ -acetone has been obtained.

Treatment of a $1 \text{ }\mu\text{M}$ solution of $\text{Cu}^{\text{II}}[\text{BOT1}]$ with 1000 equivalents of cysteine restored the emission to that of uncomplexed BOT1, owing to reduction of the paramagnetic Cu^{2+} ion. The positive ion electrospray mass spectrum of this reduced species showed a peak with $m/z = 604.3$, which corresponds to the cationic $[\text{Cu}^{\text{I}}(\text{BOT1})]^+$ complex (calcd $m/z = 604.0$) (Fig S4). A solution of $\text{Cu}^{\text{II}}[\text{BOT1}]$ in buffered aqueous solution was treated with excess Angeli's Salt, which generates an equimolar ratio of nitroxyl (HNO) and nitrite under physiological conditions.²⁴ A 4.3 ± 0.6 fold increase in emission was observed, demonstrating fast HNO detection with significant turn-on under physiologically relevant conditions (Fig. 1). Emission turn-on was visualized using as little as $50 \text{ }\mu\text{M}$ Angeli's salt. $\text{Cu}^{\text{II}}[\text{BOT1}]$ displayed a negligible change in emission when treated with a 1000-fold excess of NaNO_2 , indicating that the turn-on response induced by Angeli's Salt is due to HNO production and not the NO_2^- side product. HNO reacts with SODCu^{II} to generate NO and reduced SODCu^{I} .¹⁹ A similar reaction appears to occur with $\text{Cu}^{\text{II}}[\text{BOT1}]$, because treatment of the complex with Angeli's salt results in production of NO (g), as observed by EI-MS (Fig S5), concomitant with reduction of the paramagnetic Cu^{2+} complex to give the same $[\text{Cu}^{\text{I}}(\text{BOT1})]^+$ species observed by ESI-MS that is obtained upon reduction with cysteine (Fig S4). EPR spectroscopy provides further evidence for reduction of the paramagnetic $\text{Cu}^{\text{II}}[\text{BOT1}]$ complex by HNO (Fig S6). The emission response for $\text{Cu}^{\text{II}}[\text{BOT1}]$ is highly specific for HNO over other reactive species present in the biological milieu. Apart from NO_2^- , other RNS and ROS including NO, NO_3^- , ONOO^- , H_2O_2 , OCl^- failed to induce significant emission enhancement of the $\text{Cu}^{\text{II}}[\text{BOT1}]$ complex (Fig. 1b). The negligible emission enhancement observed upon treatment of $\text{Cu}^{\text{II}}[\text{BOT1}]$ with saturated solutions of buffered NO is especially noteworthy and makes this system potentially valuable for studying the proposed disparate roles of NO and HNO in biology.

We next assessed the ability of $\text{Cu}^{\text{II}}[\text{BOT1}]$ to operate in live cells. HeLa cells were incubated with $1 \text{ }\mu\text{M}$ $\text{Cu}^{\text{II}}[\text{BOT1}]$ (1 h, 37°C). Under these conditions, cells show only faint intracellular fluorescence (Fig. 2a). Addition of $200 \text{ }\mu\text{M}$ Angeli's salt increased the observed intracellular red fluorescence over the course of 10 min, consistent with an HNO-induced emission response. No change in emission intensity was observed for the same time period for cultures to which Angeli's salt was not added (Fig S7). Moreover, treatment of HeLa cells incubated with the $\text{Cu}^{\text{II}}[\text{BOT1}]$ probe with the NO donor diethylamine NONOate ($200 \text{ }\mu\text{M}$) did not enhance the observed fluorescence (Figure S8). Addition of exogenous cysteine ($200 \text{ }\mu\text{M}$) to cells pretreated with $\text{Cu}^{\text{II}}[\text{BOT1}]$ induced a rapid increase in emission (Fig S9), consistent with

reduction to Cu^+ . In related work, ascorbate was applied as an external reductant to image labile pools of copper.²⁵ The lack of a substantial fluorescent signal following addition of $\text{Cu}^{\text{II}}[\text{BOT1}]$ to cells assures that normal levels of intracellular cysteine and other thiols are insufficient to produce the fluorescent response that we observe for HNO.

$\text{Cu}^{\text{II}}[\text{BOT1}]$ is the first fluorescent molecular probe with visible excitation and emission profiles for detecting HNO in living biological samples. It features excellent selectivity for HNO over other biologically relevant RNS, including NO. The development of cell-trappable, longer-wavelength emission $\text{Cu}^{\text{II}}[\text{BOT1}]$ homologues aimed at unraveling the biology of HNO in living systems is in progress.

Supplementary Material

Refer to Web version on PubMed Central for supplementary material.

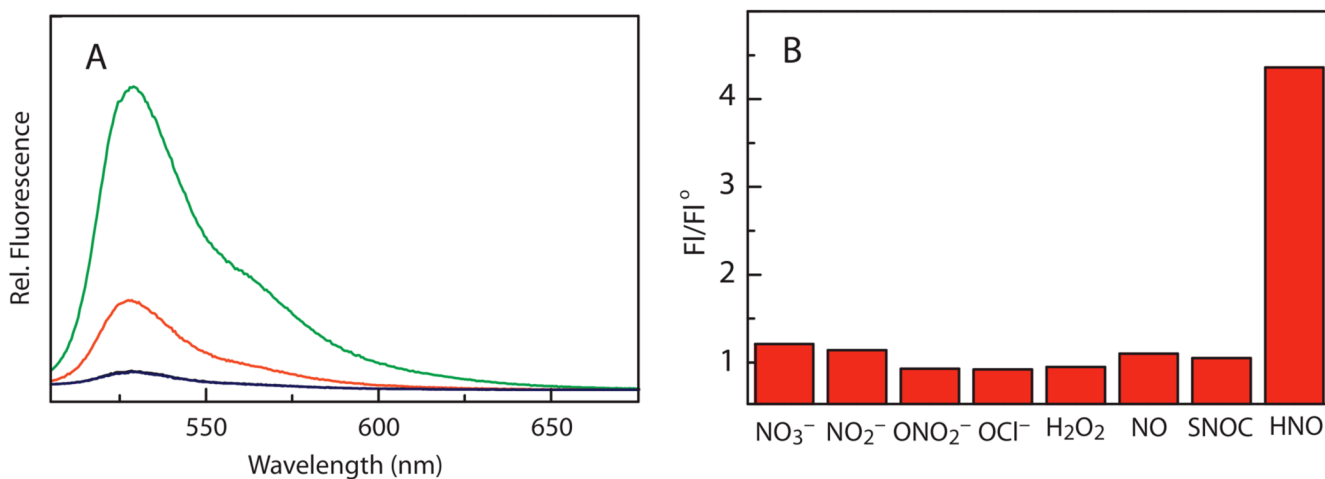
Acknowledgments

We thank Dr. Daniel A. Lutterman for assistance with fluorescence lifetime measurements and Yogesh Surendranath for help with EI-MS. JR acknowledges postdoctoral fellowship support from the NIH (F32 GM080060-02). This work was supported by NSF grant CHE-0611944.

References

1. Murad F. *Biosci. Rep* 1999;19:133–154. [PubMed: 10513891]
2. Moncada S, Palmer RM, Higgs EA. *Pharmacol Rev* 1991;43:109–142. [PubMed: 1852778]
3. Lim MH, Lippard SJ. *Acc. Chem. Res* 2006;40:41–51. [PubMed: 17226944]
4. Lim MH, Wong BA, Pitcock WH, Mokshagundam D, Baik MH, Lippard SJ. *J. Am. Chem. Soc* 2006;128:14364–14373. [PubMed: 17076510]
5. Lim MH, Xu D, Lippard SJ. *Nat. Chem. Biol* 2006;2:375–380. [PubMed: 16732295]
6. Kojima H, Nakatsubo N, Kikuchi K, Kawahara S, Kirino Y, Nagoshi H, Hirata Y, Nagano T. *Anal. Chem* 1998;70:2446–2453. [PubMed: 9666719]
7. Kim J-H, Heller DA, Jin H, Barone PW, Song C, Zhang J, Trudel LJ, Wogan GN, Tannenbaum SR, Strano MS. *Nat Chem* 2009;1:473–481.
8. Hughes MN. *Biochim. Biophys. Acta* 1999;1411:263–272. [PubMed: 10320662]
9. Irvine JC, Ritchie RH, Favalaro JL, Andrews KL, Widdop RE, Kemp-Harper BK. *Trends Pharmacol. Sci* 2008;29:601–608. [PubMed: 18835046]
10. Fukuto JM, Dutton AS, Houk KN. *ChemBioChem* 2005;6:612–619. [PubMed: 15619720]
11. Miranda KM, Paolocci N, Katori T, Thomas DD, Ford E, Bartberger MD, Espey MG, Kass DA, Feelisch M, Fukuto JM, Wink DA. *Proc. Natl. Acad. Sci. U. S. A* 2003;100:9196–9201. [PubMed: 12865500]
12. Wink DA, Miranda KM, Katori T, Mancardi D, Thomas DD, Ridnour L, Espey MG, Feelisch M, Colton CA, Fukuto JM, Pagliaro P, Kass DA, Paolocci N. *Am J Physiol Heart Circ Physiol* 2003;285:H2264–H2276. [PubMed: 12855429]
13. Ma XL, Gao F, Liu G-L, Lopez BL, Christopher TA, Fukuto JM, Wink DA, Feelisch M. *Proc. Natl. Acad. Sci. U. S. A* 1999;96:14617–14622. [PubMed: 10588754]
14. Fukuto JM, Bartberger MD, Dutton AS, Paolocci N, Wink DA, Houk KN. *Chem. Res. Toxicol* 2005;18:790–801. [PubMed: 15892572]
15. Espey MG, Miranda KM, Thomas DD, Wink DA. *Free Radic. Biol. Med* 2002;33:827–834. [PubMed: 12208370]
16. Irvine JC, Favalaro JL, Kemp-Harper BK. *Hypertension* 2003;41:1301–1307. [PubMed: 12743008]
17. Irvine JC, Favalaro JL, Widdop RE, Kemp-Harper BK. *Hypertension* 2007;49:885–892. [PubMed: 17309955]

18. Hobbs AJ, Fukuto JM, Ignarro LJ. *Proc. Natl. Acad. Sci. U. S. A* 1994;91:10992–10996. [PubMed: 7526387]
19. Murphy ME, Sies H. *Proc. Natl. Acad. Sci. U. S. A* 1991;88:10860–10864. [PubMed: 1961756]
20. Marti MA, Bari SE, Estrin DA, Doctorovich F. *J. Am. Chem. Soc* 2005;127:4680–4684. [PubMed: 15796534]
21. Tennyson AG, Do L, Smith RC, Lippard SJ. *Polyhedron* 2007;26:4625–4630.
22. Loudet A, Burgess K. *Chem. Rev* 2007;107:4891–4932. [PubMed: 17924696]
23. Huang S, Clark RJ, Zhu L. *Org. Lett* 2007;9:4999–5002. [PubMed: 17956110]
24. Liochev SI, Fridovich I. *Free Radic. Biol. Med* 2003;34:1399–1404. [PubMed: 12757850]
25. Domaille DW, Zeng L, Chang CJ. *J. Am. Chem. Soc* 2010;132:1194–1195. [PubMed: 20052977]

**Figure 1.**

(A) Fluorescence spectrum of 3 μ M BOT1 ($\lambda_{\text{exc}} = 450$ nm) in 50 mM PIPES buffer and 100 mM KCl (pH 7, 25 °C) (green), spectral changes after addition of 2 equiv of CuCl_2 to generate $\text{Cu}^{\text{II}}[\text{BOT1}]$ (blue), and subsequent addition of 1000 equiv of Angeli's salt (red). (B) Fluorescence responses of 3 μ M $\text{Cu}^{\text{II}}[\text{BOT1}]$ to various RNS and ROS 1.9 mM NO, 3.0 mM for all other RNS/ROS). Spectra were acquired in 50 mM PIPES and 100 mM KCl, pH = 7, and all data were obtained after incubation with the appropriate RNS/ROS at 25 °C for 1 h. Collected emission was integrated between 475 and 675 nm ($\lambda_{\text{exc}} = 450$ nm).

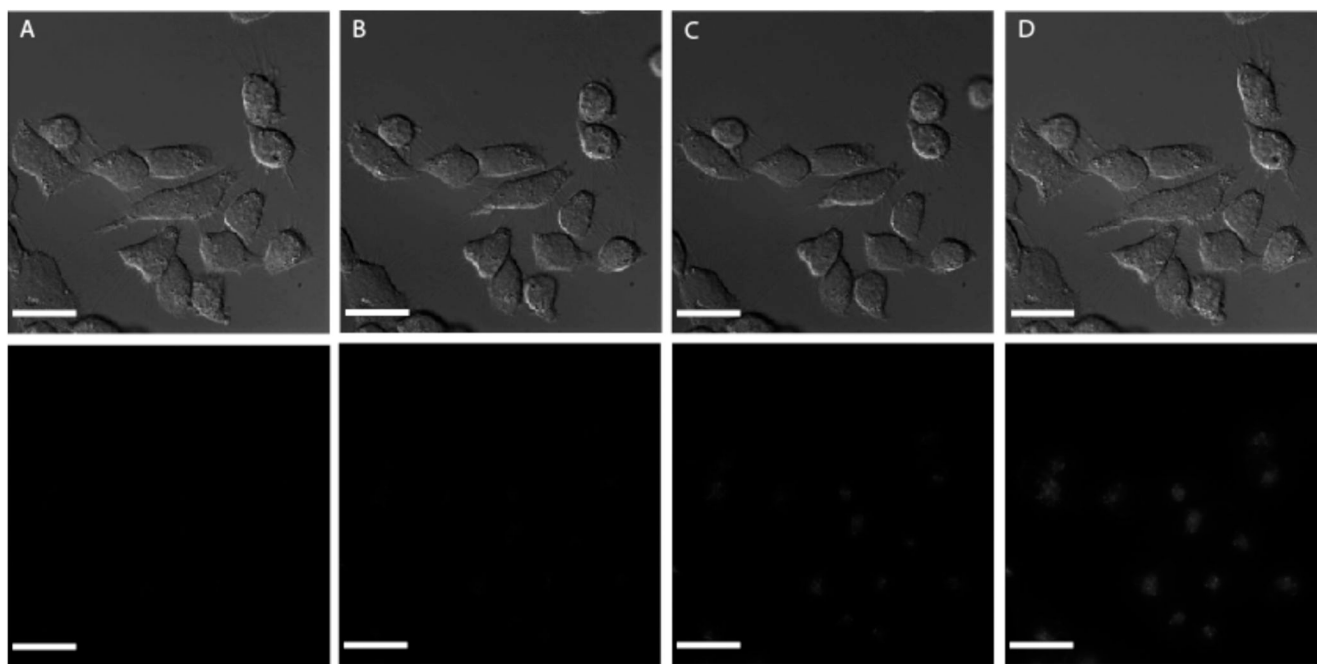
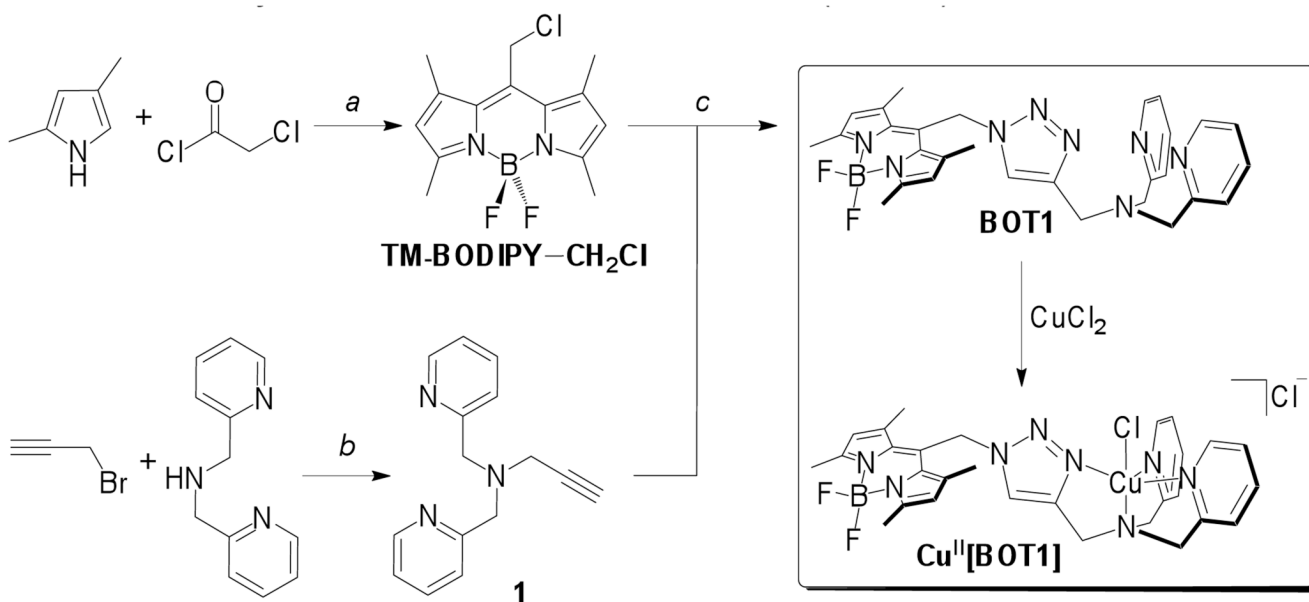


Figure 2. HNO-induced fluorescence response in HeLa cells (A) stained with 1 μM Cu^{II} [BOT1] and (B) 1 min, (C) 5 min and (D) 10 min after treatment with Angeli's salt (200 μM). (Top) DIC image, (bottom) fluorescence image. Scale bar: 25 μm .



(a) 1. O₂; 2. NEt₃; 3. BF₃·OEt₂; (b) K₂CO₃, ; (c) NaN₃, CuI, sodium ascorbate, DMSO/H₂O

Scheme 1.
Synthesis of BODIPY-triazole 1 (BOT1)